Journal of Computers Vol. 37 No. 5, October 2026, pp. 409-425
https://doi.org/10.63367/19911599202610370502 5

Deep Learning-Based Welding Process Optimization and Adaptive Control Method for Welding Robots

Hai-Tao Li[1,2], Xiao-Long Tian[1*], Peng Zhang[1],
Feng Yang[1], Tao Wang[1], and Ci-En Li[1]

[1] Hebei Mechanical and Electrical Polytechnic,
Xingtai City 054000, Hebei Province, China

lht3236@163.com, tianxiaolong@hbjd.edu.cn, zhangpeng@hbjd.edu.cn
fengfeng144@163.com, wangtao@hbjd.edu.cn, 343673291@qq.com

[2] Xingtai Technology Innovation Centre for Intelligent Welding and Cutting Engineering,
Xingtai City 054000, Hebei Province, China

Received 10 July 2026; Revised 30 July 2026; Accepted 10 September 2026

Abstract. GMAW (gas metal arc welding) robots are frequently used in contemporary manufacturing as they offer high levels of productivity, repeatable process stability and less need for manual labour. However, even today practical robotic welding is often based upon manual design, teaching and offline programming. Welding parameters and trajectories must be redesigned whenever the workpiece, joint geometries or assembly conditions change. Furthermore, during welding, changes to the weld-seam state caused by machining error, assembly deviation and cyclic heat input result in weld parameters planned for ideal conditions becoming inadequate and the risk of incomplete fusion, porosity, cracking, slag inclusions and unstable backside formations greatly increased. In this paper a method based on deep learning is presented to provide optimization of the welding process and adaptive control for GMAW robots. This method consists of integrated quality grade oriented process planning; site-specifically improved multi-objective parameter optimization; semi-supervised semantic segmentation for the perception of weld seams and molten pools and their associated spatter suppression through neural networks predicting weld formation; and fuzzy adaptive control logic. Butt joints of Q235 carbon structural steel were tested experimentally and a response surface model was developed linking welding current, welding speed, torch angle and nozzle height to geometric properties of the welds.

Keywords: GMAW, welding robot, deep learning, process optimization, semi-supervised segmentation, weld seam tracking, fuzzy adaptive control

1 Introduction

Robotic welding is not currently fully automated. Many manufacturing facilities still utilize manual teaching or offline programming to determine the welding path of a robotic welding system [1]. An experienced technician must set up welding current, voltage, speed of travel, feed rate for wire, angle of the torch, type of shielding gas and height of the nozzle based on their prior experience. If a factory introduces new workpieces or joint configurations, a new set of parameter values and the path of travel for weld must be created [2]. All of the preparation time necessary to do this creates significant reliance on experienced robotic welding engineers. This reliance is even more acute for batch sizes less than ten, complex joint configurations, and constantly changing assembly conditions when a robot is required to perform numerous different tasks in succession [3]. Another obstacle is the fluctuating nature of the welding process. During automated welding processes, the weld seam does not remain constant. The dynamic behaviour of the torch when welded could result from machining, fixture and/or gap discrepancies, heat-induced deformations, and heating up of the work piece [4]. Over time, if the robotic system continues to execute its preprogrammed trajectory and parameters, the parameters defined for a given welding process will move further away from the actual weld. Mismatches between the actual weld and desired weld could lead to problems such as inappropriate molten pool characteristics and excessive spatter. This, in turn, could lead to problems such as lack of penetration or reinforcement and lack of backside fusion [5].

* Corresponding Author

Therefore, improving GMAW using robots will require both off-line parameter optimization and on-line sensing, visual assurance and adaptive quality control of the entire process. Advances in three areas of technology provides opportunities to overcome some of these challenges: computer vision; deep learning; intelligent optimization and modelling using fuzzy logic [6]. Using deep semantic segmentation will enable extraction of certain features from welding images that are impacted by inherent noise. Semi-supervised learning techniques can be beneficial since they are typically time-consuming and costly to generate pixel-level welding labels [7]. In addition, neural networks can be used to create nonlinear models of the relationships among the process inputs, molten pool characteristics and a welded part's geometry. The purpose of this article is to create an English scientific manuscript based on a doctoral study investigating intelligent process planning and adaptive control of weld quality in GMAW robots. The doctoral study created a robotic GMAW experimental platform, compiled welding process and visual experience data, optimized GMAW parameters for various joint quality grades, created a semi-supervised segmentation method for weld tracking and spatter suppression, and created a neural-network-fuzzy controller for adjusting the formation of welds [8]. This article will reorganize the above technical components into a welding process optimization and an adaptive control system based on deep learning that is suitable for SCI-style publication in Fig. 1.

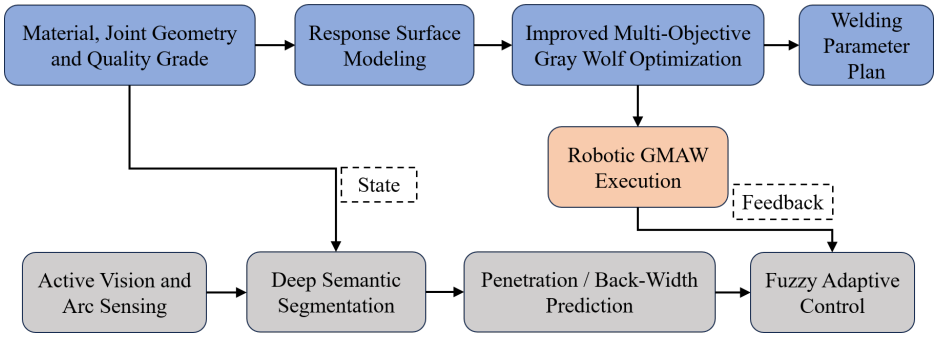


Fig. 1. Integrated framework of the proposed deep learning-based robotic GMAW optimization and adaptive control method

2 Materials, Experimental Platform and Data Acquisition

2.1 Materials and Joint Configuration

The experimental object is Q235 carbon structural steel, a widely used structural material in buildings, bridges and mechanical equipment. The filler wire is ER70S-6, which is commonly used in GMAW of carbon steel. Before welding, the butt-joint surfaces are mechanically polished to remove oxide scales and impurities so that the influence of surface contamination on weld formation is reduced. The experimental plates have a dimension of 200 mm × 100 mm × 3 mm, the wire diameter is 1.2 mm, and the butt-joint gap is set to 1.4 mm. This configuration allows the study to focus on the relationship between welding process parameters, weld geometry, visual weld-state information and joint formation quality in Table 1. The choice of Q235 steel is meaningful because it represents a typical industrial carbon structural steel. Its weldability is suitable for studying both process planning and process control. In addition, the plate thickness of 3 mm makes the back-side fusion width and penetration depth sensitive to heat input, torch position and molten-pool behavior. These characteristics provide an appropriate test condition for evaluating intelligent planning and adaptive control methods in Table 2.

Table 1. Chemical composition of base metal and filler wire

Material	C	Mn	Si	Cr	Ni	P	S	Fe
Q235 plate	0.167	0.284	0.162	0.0186	0.0042	0.0205	0.0096	Bal.
ER70S-6 wire	0.06-0.15	1.40-1.85	0.80-1.15	≤0.025	≤0.035	-	-	-

Table 2. Mechanical properties of Q235 steel plate

Material	Yield strength (*Mpa*)	Tensile strength (*Mpa*)	Uniform elongation	Fracture elongation	Vickers hardness (*HV*)
Q235	220-240	400-420	14.7%	28.3%	206.19

2.2 Robotic GMAW Platform

A welding platform composed of 4 distinct subsystems, namely; welding subsystem, robot sub-system, visual sensing subsystem, and a control subsystem that is computer based [9]. The robotic subsystem includes a six axis industrial robot (ABB IRB1410). The robot is fitted with a GMAW welding torch and executes the welding path dictated by commands sent by the upper computer and the robot controller. The repeatability of the robot of 0.05mm ensures sufficient positioning accuracy for the automated butt-welding of components. The robotic welding subsystem consists of a fully digitally controlled welding power source, a wire feeder, shielding gas supply, a water cooled robotic welding torch, and a torch cleaning station [10]. The welding power source communicates with the robot controller using an industrially defined communications protocol, allowing the control subsystem to command the welding process and to receive current and voltage readings from the welding process. The wire feeder provides accurate and stable wire feeding over a large range of wire feed speeds, and the TBi Robotics RM2 Water-Cooled Robotic Welding Torch provides excellent tool centre point (TCP) stability [11]. The control subsystem is connected to the robot system through Ethernet, and it coordinates the completion of welding processes, the acquisition of welding images, and the correction of trajectories, and the adjustment of process parameters. An active laser-based vision sensor is mounted adjacent to the welding torch in an eye-in-hand design. This configuration is space-efficient and ensures that no occlusion is generated as the robot moves down the weld seam. The image sensor is comprised of the camera, lens, narrowband optical filter and a 650 nm line laser. During the welding process, the sensor captures images which include weld seams, laser stripes, molten pools, spatter and distorted locations. These image coordinates are then transformed to robot coordinates to allow for the use of visual features for both path correction and control of the welding process while it is being performed in Fig. 2 and Table 3.

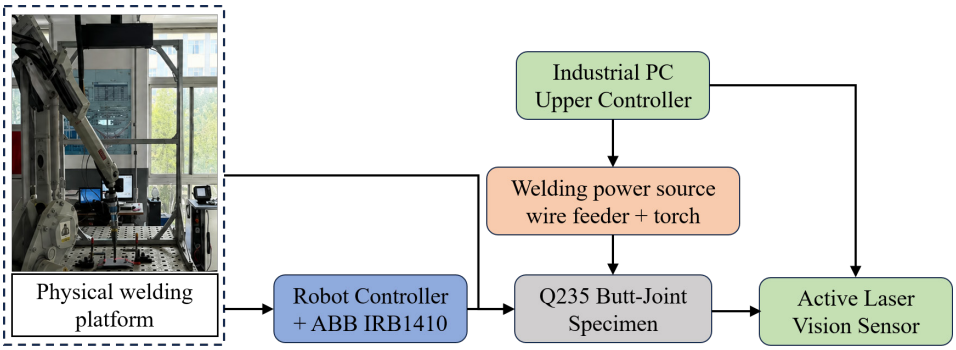


Fig. 2. Experimental platform and sensing architecture for robotic GMAW

Table 3. Main experimental equipment and sensing components

Subsystem	Main component	Key specification
Robot	ABB IRB1410	6 axes, 5 kg payload, 0.05 mm repeatability
Power source	Artsen II CM350	Digital GMAW power source, 50-500 A, 12-50 V
Wire feeder	WF1-50Z	1.4-24 m/min wire-feeding speed, 0.8-1.6 mm wire
Torch	TBi RM2	Water-cooled robotic torch, 20 mm nozzle
Camera	ME2P-1230-9GC-P	4096 × 3000 resolution, RJ45 interface
Laser	FU650AB100-GD16	650 nm line laser with Powell prism

3 Quality-Grade-Oriented Welding Process Optimization

3.1 Welding Quality Grade and Response Variables

Quality assessments of welds are done from the outside and for how sound the internal joints are. Companies will generally use visual inspection and geometric factors to determine if the process is acceptable to perform the task but use other Non Destructive Testing (NDT) methods for detection of flaws once the joint has been made [12]. The original study used ISO 5817:2023 as the reference for quality grades of steel fusion welded joints. The grades can be further categorized as B, C & D grades whereby B is the highest grade produced, used for critical structural applications, C is for high strength and non-critical structures, and D is the minimum acceptable quality level produced, used for non-structural applications. The present framework has established quality-grade constraints when optimizing the process so that the robot will not always produce a totally optimal set of parameters for a given process but will generate an application-specific set of process parameters based on the desired weld quality grade. In this study, the welding power supply is operated in a synergistic manner such that the voltage and wire feed speed will be automatically adjusted to the set current. The shielding gas flowrate will be constant during the welding process, and the established flowrate equals 18 L/min. Responses from the welding process include penetration of the weld, upper reinforcement, undercut, the weld width, the backside fusion width of the weld, and the weld toe angle. Each of these responses has a direct correlation with ISO standards for quality, appearance of the weld, and the reliability of the joint for load carrying functions in Table 4.

Table 4. Welding variables and quality-response indicators

Variable group	Variables or indicators	Role in the study
Input parameters	Current, welding speed, torch angle, nozzle height	Decision variables for process planning and adaptive control
Fixed conditions	Shielding gas flow, plate thickness, wire type	Experimental consistency and baseline welding condition
Weld geometry	Penetration depth, reinforcement, undercut, weld width, back-side width, toe angle	Response variables for quality grade and optimization
Quality grade	B, C and D according to ISO 5817	Constraint condition for intelligent process planning

3.2 Response Surface Model and Heat-Input Interpretation

There are no consistent relationships between welding parameters and weld geometries as current is increased, generally, the amount of arc heat input and melting capabilities will also increase; as welding speed is increased, the amount of heat input will decrease on a per-unit-of-length basis; and, torch angle, as well as nozzle height, will cause variation in arc force, shape of molten pool, tendency toward spatter and how heat is distributed both sides of the groove. Subsequently, to develop a model for quantitatively planning an efficient process; a second-order regression model is developed to fit each weld response with respect to process variables as well as the interaction of those variables, using preliminary experimental data to establish each of these functions [13]. In this case, heat input serves as the physical basis upon which to interpret the effects of current, voltage & travel speed and will be demonstrated through the heat input equation in equation (1) where the combination of efficiency, voltage, current, and travel speed determines the thermal energy applied to a weld; excessive heat input can result in either molten pool collapse with excessive penetration or porosity; insufficient heat input can result in either incomplete fusion with lack of penetration.

$$H = \eta \frac{UI}{v} \tag{1}$$

The response surface model in equation (2) is used to describe the relationship between process inputs and weld geometric outputs. This model enables the system to predict whether a candidate parameter set can satisfy quality-grade constraints before physical welding is performed [14].

$$y = \beta_0 + \sum_{i=1}^{k} \beta_i x_i + \sum_{i=1}^{k} \beta_{ii} x_i^2 + \sum_{i \le j} \beta_{ij} x_i x_j + \zeta \tag{2}$$

3.3 Multi-Objective Optimization and Intelligent Planning

Multi-objective optimization creates a plan to manage how multiple goals interact during welding. The multiple goals include getting both sufficient penetration at the front and enough weld bead width without excessive reinforcement or undercutting, minimizing wasted material, and optimizing the performance of the welding operation [15]. The limitations on the allowable geometric dimensions to yield a particular quality of produced welds vary depending upon the degree of quality required. This makes the search region of the solution space dependent on the target quality of the weld as well. Therefore, the planning model searches through the parametric space to generate feasible combinations of welding parameters which satisfy the various constraints of each combination, and selects a single combination from amongst the various combinations found in terms of producing a weld, according to the principle of maximum efficiency [16]. The multi-objective gray wolf optimization (GWO) algorithm was used to search the feasible region within the parameterization space (GWO). Each candidate solution was represented by a wolf and each wolf's position represented a combination of the welding parameters. Similarly, each of the best candidate solutions provided to the wolves will lead or migrate to lead the populations of wolves toward the Pareto front of all candidates. Compared with trial and error, GWO eliminates the requirement for technicians to estimate correct parameters because GWO will reduce the number of test trials and cut the cost of experimental testing. The multi-objective nature of the project specification is defined in mathematical formational terms according to equation (3) and the parametric updating mechanistically of GWO candidates is described in equation (4) in Fig. 3.

$$\min F(X) = \{f_1(X), f_2(X), \ldots f_s(x)\} \tag{3}$$

$$\vec{D} = \vec{C} \cdot \vec{X}_p(t) - \vec{X}(t) \tag{4}$$

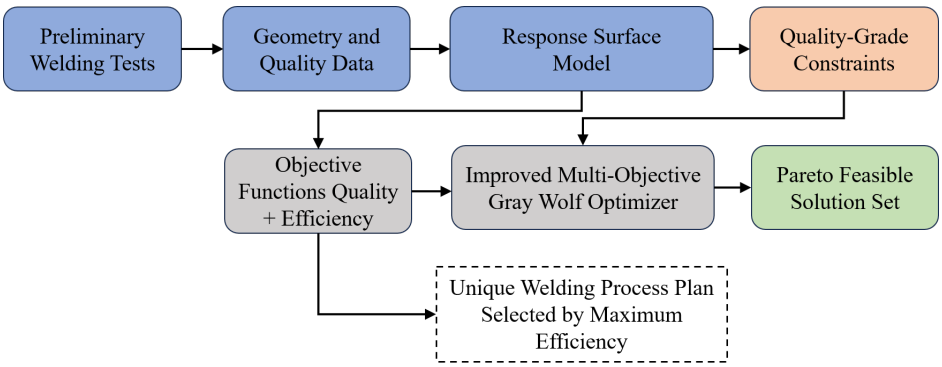


Fig. 3. Intelligent GMAW process planning based on response modelling and multi-objective optimization

The optimization results reported in the source investigation show that the process planning method can prepare welded joints for different quality levels and that heat input differences among quality grades produce different microstructures and mechanical properties. Compared with the base material hardness, the peak hardness of three quality-grade joints increased by 30.72%, 40.86% and 51.74%, respectively. Yield strength increased by 7.97%, 5.31% and 3.97%, while tensile strength increased by 3.82%, 3.19% and 1.36%. These results indicate that quality-grade-oriented planning does not merely select arbitrary parameter values; it links process parameters with weld formation and joint properties.

4 Deep Learning-Based Weld Seam Tracking and Spatter Suppression

Part 4 proposes a semi-supervised visual perception method for robotic GMAW. The method employs an improved U2PL network, integrating a ResNet101 encoder, a DeepLabV3+ decoder, a momentum teacher mechanism, pseudo-label learning, contrastive loss, and affinity field loss, to segment weld seams, laser stripes, spatter, molten pools, and deformation points from complex welding images [17]. The dataset comprises 553 annotated and 846 unannotated images; the training process incorporates data augmentation, SGD optimization, an ASPP module, EMA, and a polynomial learning rate decay strategy. The resulting visual outputs are utilized for weld seam tracking, deviation correction, and spatter analysis. The method achieves an mIoU of 85.72%, outperforming GTA and DeepLabV3+.

4.1 Semi-Supervised Semantic Segmentation Network

The visual sensing method can help to address the limitations of offline teaching and programming [18]. One challenge faced when trying to build a welding database from welding images is the arc light, reflections, and other elements of the welding process, which will all affect image quality and therefore make them suitable for computer based analysis. Building a fully supervised segmentation model requires many pixel level labels, and the cost of annotating welding images is typically very high; consequently developing a semi-supervised segmentation model using the U2PL semi-supervised segmentation network will reduce the cost of labeling while potentially increasing the robustness of the model. The network developed will utilise a momentum based teacher network that is maintained along with a student network through the use of an exponential moving average from the student to the teacher networks; therefore the model will learn from unlabeled images by generating pseudo labels for these images using the trained teacher network. The encoder is based on the ResNet101 architecture, while the decoder consists of the deepLabV3+ architecture. Atrous convolution will be added to the encoder to enhance the size of the receptive field without significantly increasing the number of parameters in the model; therefore it will allow the network to perceive small and widely dispersed spatter, thin laser stripes, as well as large molten pool regions simultaneously. All but one of the batch normalization layers in the model architecture have been changed to use synchronised batch normalisation such that the network can be trained across multiple devices in a distributed fashion; the remaining batch normalisation will remain as standard batch normalisation to ensure the model is stable during training. The final model architecture can be seen in Fig. 4. The final loss function combines supervised loss on labeled data, unsupervised pseudo-label loss on reliable unlabeled predictions, contrastive loss for uncertain regions, and affinity-field loss for boundary continuity. The total loss is defined in equation (5). The affinity component strengthens spatial consistency between adjacent pixels, which is especially useful for weld seam edges and irregular spatter boundaries.

$$L_A = L_s + \lambda_u L_u + \lambda_c L_c + \lambda_a L_a \tag{5}$$

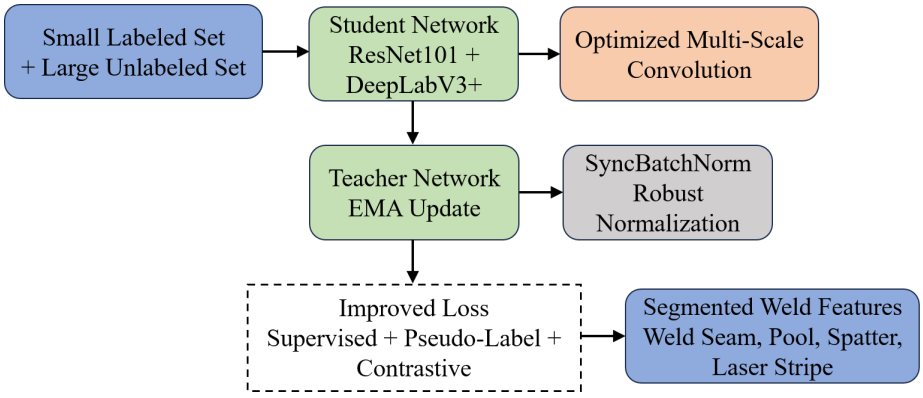


Fig. 4. Improved U2PL semi-supervised segmentation architecture for welding images

For the unlabeled welding image x_i^u, the teacher network first predicts the class probability distribution. The class with the highest probability is selected as the pseudo-label [19]. To avoid introducing unreliable supervision, only pixels whose prediction confidence is higher than the threshold are used for unsupervised training:

$$\hat{y}_i = arg\ \max_c P_t(c \mid x_i^u) \tag{6}$$

$$m_i = I(\max_c P_t(c \mid x_i^u) \geq \tau) \tag{7}$$

Where $\hat{y}_i$ denotes the pseudo-label, $P_t(c \mid x_i^u)$ denotes the prediction probability of the teacher network for class c, and m_i is the confidence mask. The teacher network is updated by the exponential moving average of the student network parameters. This strategy can stabilize pseudo-label generation and reduce the influence of noise during training:

$$\theta_t^k = \alpha\theta_t^{k-1} + (1-\alpha)\theta_s^k \tag{8}$$

Where θ_t^k and θ_s^k are the parameters of the teacher network and student network at the k-th iteration, respectively. α is the momentum coefficient.

4.2 Dataset, Training and Evaluation

The robotic GMAW image database has been populated with images taken from 27 different welding parameters. There were 553 labelled images and 846 unlabeled images in the dataset after post-processing such as image selection, cropping and augmentation. The image size is set to 600 by 600 prior to any training/processing. The classes annotated are; weld seam, laser stripe, spatter, molten pool, and distortion point. Random image augmentations employed in this study included; random scaling, random cropping, random flipping, Gaussian blur, and CutMix. These augmentations allow the dataset diversity to be enhanced and provide a force for the network to learn features that are resilient to local occlusion and image discontinuity. The underlying computational network is built on the PyTorch framework. The encoder of the model uses a ResNet101 network pre-trained on ImageNet as the initialisation point for transfer learning. The optimizer for training is stochastic gradient descent (SGD) with an initial learning rate of 0.001, weight decay 0.0001, and momentum 0.9; the DeepLabV3+ model makes use of 3 dilation rates (12, 24 and 36) as part of its atrous spatial pyramid pooling module. A polynomial decay schedule was used for the learning rate, and the teacher network was updated using the exponential moving average method. The performance of the model was evaluated using the mean intersection over union defined and in Table 5.

$$mloU = \frac{1}{k+1}\sum_{i=1}^{k}\frac{TP_i}{TP_i + FP_i + FN_i} \tag{9}$$

The learning rate was updated by a polynomial decay strategy during training, which gradually reduced the learning rate as the number of iterations increased. This strategy helps stabilize the later stage of network optimization and prevents large parameter oscillations near convergence. The learning rate at iteration t is expressed as:

$$\eta_t = \eta_0(1-\frac{t}{T})^p \tag{10}$$

Where η_t is the learning rate at iteration t, η_0 is the initial learning rate, T is the total number of training iterations.

Table 5. Dataset and training settings for the segmentation network

Item	Setting
Labeled images	553
Unlabeled images	846
Image size	600 × 600
Classes	weld seam, laser stripe, spatter, molten pool, distortion point
Encoder	ResNet101
Decoder	DeepLabV3+
Optimizer	SGD, learning rate 0.001, momentum 0.9
ASPP dilation rates	12, 24, 36
Evaluation metric	mIoU

4.3 Visual Guidance, Deviation Correction and Spatter Model

During welding, the laser vision system detects weld seam position ahead of the current torch position [20]. Because the robot motion and actual welding point may have tracking deviations, the detected seam coordinate is corrected by the current x-direction and y-direction deviations before being transmitted to the robot controller. This correction strategy allows the robot to follow a continuously varying butt seam rather than a fixed prerecorded path. Spatter is also considered in the control strategy because excessive high-brightness spatter deteriorates surface quality and increases post-weld cleaning. Based on 27 groups of welding images, the average number of high-brightness spatter particles is fitted using multiple regression. After removing insignificant terms, the regression model in equation is obtained, where current, welding speed, torch angle and nozzle height are denoted by A, B, C and D. The model indicates that torch angle and nozzle height have strong effects on spatter quantity, and therefore these two parameters can be adjusted during spatter suppression while preserving the heat-input level required for weld formation in Fig. 5 and Fig. 6.

$$Q = -29.016 + 0.211A - 0.269B + 0.367C + 0.835D + 0.012AC - 0.031BC \tag{11}$$

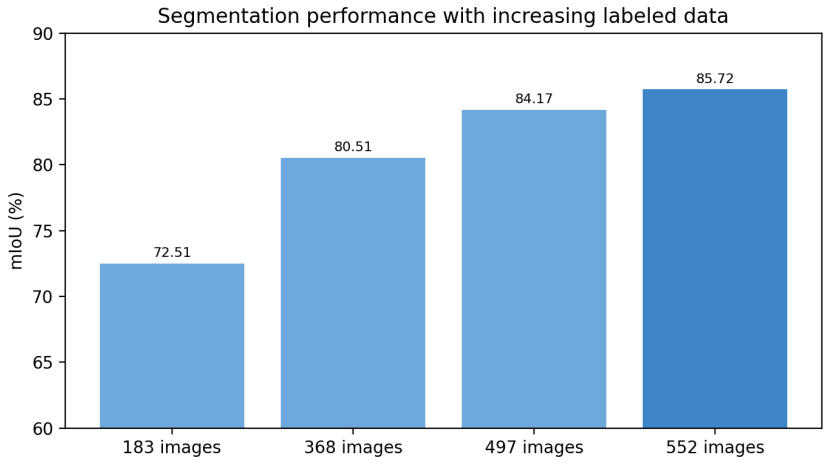


Fig. 5. Segmentation mIoU under different labeled-data sizes

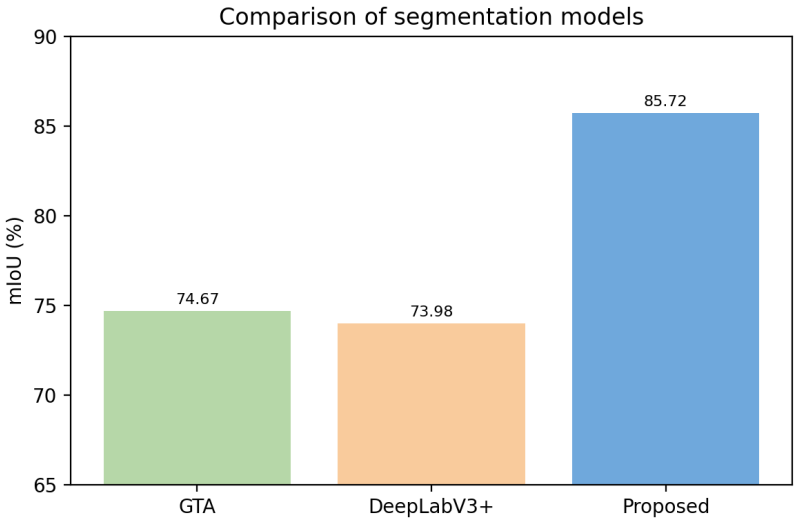


Fig. 6. Comparison between the proposed method, GTA and DeepLabV3+

The proposed segmentation method reaches an mIoU of 85.72%. Under the same dataset condition, it improves mIoU by 11.05 percentage points compared with GTA and by 11.74 percentage points compared with fully supervised DeepLabV3+. This improvement confirms that the semi-supervised strategy and architecture modifications are suitable for welding scenes with limited labeled data and complex visual disturbances in Table 6.

Table 6. Segmentation performance of different training settings and models

Model or dataset setting	mIoU (%)
183 labeled images	72.51
368 labeled images	80.51
497 labeled images	84.17
552 labeled images	85.72
GTA model	74.67
DeepLabV3+	73.98
Proposed improved U2PL	85.72

5 Neural-Network Prediction and Fuzzy Adaptive Control

5.1 Weld Formation Prediction Model

The penetration depth and back side fusion width are the primary parameters used to assess the quality of butt joint formations and parameters that affect the values of these two parameters such as the molten pool state, as well as process variables [21]. Therefore, a prediction model will be created that combines data from both process variables and visual features; current, welding speed, torch angle, nozzle height, molten pool long semi-axis and short semi-axis will serve as input variables with penetration and back side fusion width as output variables [22]. While both least squares regression and BP neural network are assessed during the original work, BP neural network is selected as the preferred method due to the ability of the neural network to capture non-linear relations of process variables to torch posture and molten pool geometry. The general expression for the neural mapping can be seen in equation; 8 hidden neurons provide an adequate level of error to time ratio for

penetration, while 9 hidden neurons provide an adequate level of error to time ratio for back side fusion width. The maximum absolute penetration error for the BP model is 0.4802 mm, minimum penetration error is .006 mm, and average penetration error is 0.2402 mm (see Table 7). The maximum absolute back side fusion width error is 0.4536 mm, the minimum back side fusion width error is 0.0029 mm, and the average back side fusion width error is 0.2236 mm (see Table 7).

$$\hat{Z} = \Phi(\sum_{j=1}^{m} w_j \Phi(\sum_{j=1}^{n} v_{ij} x_i + b_j) + b_o) \tag{12}$$

Table 7. BP neural network prediction performance for weld formation parameters

Output variable	Selected hidden neurons	Maximum absolute error (mm)	Minimum error (mm)	Average error (mm)
Penetration depth	8	0.4802	0.0060	0.2402
Back-side fusion width	9	0.4536	0.0029	0.2236

5.2 Fuzzy Adaptive Controller

Using its neural network prediction, the adaptive controller can adapt weld parameters in real-time [23]. This allows it to ensure a sufficient amount of penetration and the required amount of fusion width on the backside, even if there is deviation in the assembly and thermal disturbance during the welding process. As a result, there are two controlled variables evaluated and adjusted during the welding process: penetration depth and back-side width. The following three variables will be adjusted during the welding process: current, torch angle, and nozzle height. The only constant variable during the welding process is the welding speed, which allows the welding process to remain stable. Primarily, the method of adjusting the amount of heat-income is via adjusting current and adjusting the torch1s position. Since there are two controlled variables involved, the two errors in prediction must be combined to create an overall error term. The overall error term is defined as equation (9), and uses both the predicted penetration and predicted back-side width in order to calculate the total error value against their desired targets. The fuzzy controller's inputs are the fused error term and the rate of change of the fused error term. In order to construct a fuzzy-rule base for the fuzzy controller, it is necessary to define the different linguistic terms for the errors. The fuzzy-variable terms are as follows: negative big, negative medium, negative small, zero, positive small, positive medium, and positive big. A triangular membership-function was used to create the fuzzy variables, due to it being simple and providing computational-efficiency. Following the conclusion of fuzzy-inference, the fuzzy output set was converted to a crisp value, using weighted-average defuzzification in Table 8.

$$e_f = \alpha_p(\hat{p} - p^*) + \alpha_b(\hat{b} - b^*) \tag{13}$$

$$\mu(x; a, b, c) = \max(0, \min(\frac{x-a}{b-a}, \frac{c-x}{c-b})) \tag{14}$$

$$u = \frac{\sum_{i=1}^{m} v_i k_i}{\sum_{i=1}^{m} k_i} \tag{15}$$

Table 8. Main design settings of the fuzzy adaptive controller

Fuzzy component	Description
Input variables	Fused error and error variation
Output variables	Adjustment of current, torch angle and nozzle height
Error universe	-3 to 3
Current adjustment range	-40 A to 40 A
Torch angle adjustment range	-10° to 10°
Nozzle height adjustment range	-10 mm to 10 mm
Membership function	Triangular function
Defuzzification method	Weighted average

6 Results and Discussion

This intelligent robotic GMAW framework integrates process planning, visual perception, weld bead formation prediction, and adaptive control into a closed-loop architecture. The process planning module selects parameter combinations based on material, joint geometry, and quality requirements, thereby avoiding the limitations associated with seeking a single "universal optimum." [24] By holistically considering heat input, weld geometry, hardness, tensile strength, and elongation, the method effectively aligns parameter optimization with actual joint performance. The visual guidance module employs semi-supervised deep learning to segment weld seams, laser stripes, molten pools, spatter, and deformation points, enabling real-time seam tracking and trajectory correction despite assembly errors or thermal deformation. The adaptive control module combines BP neural network prediction with fuzzy control rules to estimate joint penetration and back-bead width, dynamically adjusting welding parameters in a safe and interpretable manner. Unlike traditional "teach-and-playback" welding, the robot functions not merely as an actuator repeating pre-programmed motions, but as a system capable of sensing and responding to process variations during welding. This hierarchical architecture also facilitates industrial implementation, allowing factories to adopt offline planning, visual tracking, and online control technologies in a phased manner. Overall, the framework enhances system robustness, reduces the need for repetitive teaching and trial-and-error testing, and offers a practical, low-uncertainty pathway for modern factories to achieve intelligent, flexible, and quality-focused robotic GMAW production.

6.1 Process Planning and Joint Properties

The intelligent process planning module produces multiple sets of parameters for different types of quality grades [25]. This is important because traditional optimization methods try to find the one best combination of parameters without considering the different application scenarios. A critical load-bearing joint in manufacturing might not need the same quality grade as an auxiliary structural joint. Using too much heat input and being too strict with all the joint parameters may lead to decreased production efficiency by wasting energy and filler materials. Therefore, the quality-grade-based process planning strategy provides a flexible and more useful manufacturing process design method. The test data from the previous study indicates that the optimized process parameters can create welded seams that correspond to different quality grades. When tested--microstructure examination and mechanical property testing--the amount of heat input supplied to each grade of weld has an effect on hardness; tensile strength; and elongation. The increase in the hardness of molten weld pool and the heat affected zone means that there was substantial microstructural change within the weld pool during the weld and the heat affected zone after cooling down to approximately the same temp. as the base metal prior to weld. Low elongation of the weld pool compared to the base metal indicates an increase in strength and hardness but a reduction in ductility due to the thermal cycle of the weld. The aforementioned results demonstrate the need for the integration of geometric constraints with mechanical property evaluations when planning processes for robotic welding. To select welding parameters for different quality grades, geometric and mechanical indicators should be considered simultaneously. Therefore, a grade-oriented evaluation function can be defined as:

$$F_g = w_1 \frac{B - B_g}{B_g} + w_2 \frac{P - P_g}{P_g} + w_3 \frac{\sigma - \sigma_g}{\sigma_g} + w_4 \frac{\delta - \delta_g}{\delta_g} \tag{16}$$

Where F_g is the evaluation value for quality grade g, B is the weld width, P is the penetration depth, σ is the tensile strength, and δ is the elongation.

6.2 Vision-Guided Welding Performance

A visual perception module that utilises deep learning techniques has been developed to accurately analyse and segment welding features down to the pixel level. The segmentation accuracy improves as the size of the labelled image dataset grows, from 183 to 552. Furthermore, the model benefits from the inclusion of an additional number of unlabeled images through semi-supervised learning, providing it with a higher mean Intersection-over-Union value than both the GTA model and the DeepLabV3+ model [26]. The segmentation output is used as an input to the robot so that it can (1) identify the location of the weld seam, (2) locate the laser stripe on the surface and (3) detect the location of the molten pool and high-brightness spatter. The outputs provide inputs for seam tracking, path correction and spatter control for the robot. The visual guidance approach eliminates one of the main limitations of traditional, teacher-apprentice based welding; the robot will use the detected weld seam location and then make adjustments to its path of welding while welding. This is critical in instances where the gaps in butt joint or the positioning of the plates or thermal distortion change while performing the welding process. Additionally, the spatter model further improves the quality of welds by using the visual representation of spatter to provide feedback to the welding machine. Since high-brightness spatter is heavily influenced by the angle of the welding torch and the height of the welding consumable, the robot can use the spatter model to eliminate spatter from occurring without creating needless, unnecessary disruptions to the heat input.

6.3 Adaptive Weld Formation Control

The Adaptive Quality Control Loop consists of the BP-Prediction Model and Fuzzy Controller working together to provide a combined solution. The BP-Prediction Model makes predictions of the penetration and back-side fusion widths based on both the process and characteristics of the molten, while the Fuzzy Controller uses the prediction error to make real-time adjustments. The Neural Network has an advantage against purely analytical models because it can more accurately recognize nonlinear relationships that are common in asymmetric angular root welding. In addition, there is greater interpretability for fuzzy control due to the fact that the Rules or Rule Base are similar to what an experienced welder uses to think about the process. For example, if a welder notices that the molten pool has become too large, they will reduce the amount of heat being introduced; conversely if the molten pool has become too small, they will increase the amount of heat being introduced. The results from the Control Experiments clearly show that the developed fuzzy controller can keep the back-side fusion width error within ±0.5 mm of the target value, while achieving the desired penetration depth. This is very significant because the back-side fusion width is an extremely important indicator of the quality of a weld in the Butt-Weld Root. A stable back-side fusion width indicates that there has been sufficient penetration without excessive burn-through or collapse. Thus, the combination of Neural Prediction and Fuzzy Control provides an effective method of controlling weld quality in real-time under continuously changing seam conditions, as shown in Fig. 7.

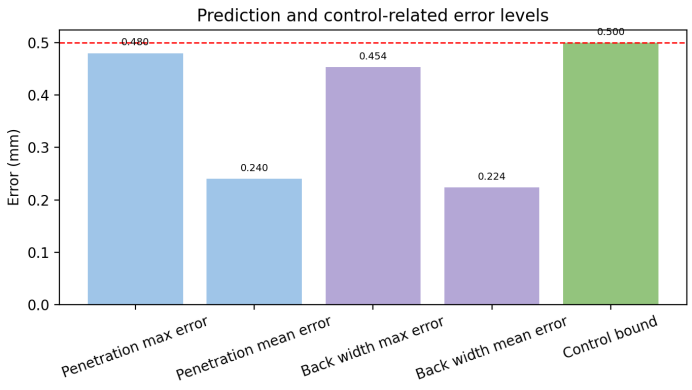


Fig. 7. Summary of neural prediction and control-related error levels

6.4 Engineering Implications

The proposed framework has several engineering implications. The first implication deals with process planning, as it should be linked to information about materials, joint geometry, and quality grades. One optimal set of parameters will not suffice; welding needs vary according to how each structure is used. The second implication has to do with the use of perception-driven trajectory correction in place of exclusively using teaching/playback for robotic welding. Visual seam tracking has the potential to reduce the impact of assembly errors and thermal distortion on the welding process significantly. The third implication has to do with combining sensor information, predictive models, and interpretable control rules for monitoring the quality of welds. The neural network can provide a nonlinear algorithm, whereas fuzzy control provides stable and intelligible decision-making capabilities. Industrial applications could implement all three layers of the system independently. The first layer would consist of an offline process-planning database and a response surface model. The second layer consists of a vision-guided tracking system based on a semi-supervised trained segmentation network. The third layer consists of online predictions of weld formation and adaptive control. Layered implementation allows for less complication when developing digitally, and allows companies to incrementally increase the intelligence of their robotic welding systems. The planning model can reduce setup time for high-volume production, while the vision and control modules will reduce the need to teach repeatedly and increase adaptability in low-batch production in Table 9.

Table 9. Engineering implementation layers of the proposed intelligent robotic welding framework

Layer	Main function	Core methods	Required inputs	Expected engineering benefit
Layer 1: Offline process planning	Select initial welding parameters according to joint and quality requirements	Process-planning database, response surface methodology, multi-objective optimization	Material type, plate thickness, groove geometry, weld quality grade	Reduces trial-and-error testing and shortens setup time
Layer 2: Vision-guided trajectory correction	Detect weld seam position and correct welding trajectory in real time	Visual seam tracking, laser vision, semi-supervised segmentation network	Welding images, laser stripe features, seam and molten pool information	Reduces the influence of assembly errors, gap variation, and thermal distortion
Layer 3: Online quality prediction and adaptive control	Predict weld formation and adjust process parameters during welding	BP neural network, fuzzy control rules, closed-loop feedback	Process parameters, molten pool geometry, penetration depth error, back fusion width error	Improves weld consistency and adaptability under changing welding conditions
Integrated system	Coordinate planning, perception, prediction, and control	Layered intelligent architecture	Offline knowledge and real-time sensing data	Supports incremental development of intelligent robotic welding systems

6.5 Additional Technical Discussion and Generalization

The proposed framework should be viewed as an integrated intelligent architecture for welding, rather than a single algorithm. Its performance depends on the consistency among four modules: process planning, visual perception, forming prediction, and controller execution. The isolation of any module will weaken the intelligence of the entire system [27]. For example, optimized process parameters can provide good initial conditions, but cannot compensate for weld displacement caused by assembly errors. Similarly, depth vision segmentation can identify weld and molten pool features, but without a controller, these features cannot be translated into process improvements [28]. Therefore, the significance of this framework lies in its closed-loop structure: offline knowledge is used to initialize the process, welding status is updated in real time, predictive models estimate hidden forming indicators, and fuzzy control transforms quality errors into executable parameter

corrections. Response surface methodology plays an important role in reducing the number of actual welding tests. Welding tests are costly because each combination of parameters requires material preparation, welding, cutting, measurement, and sometimes mechanical testing. By fitting the weld geometry response from the design experiment set, the model can make a continuous approximation of the parameter-response space. An improved multi-objective gray wolf optimization algorithm searches this space under quality level constraints. From an engineering perspective, this means that welding robots can select the process based on the required joint grade without requiring operators to perform repeated trials. This approach is particularly important for factories that frequently produce similar carbon steel parts but must adjust plate thickness, bevel gaps, or quality requirements [29]. The visual perception module is also suitable for industrial environments with relatively small amounts of data. Welding scenes are difficult to label because the boundaries between the molten pool, arc light, spatter, and laser stripes change rapidly. Fully supervised methods may perform well on laboratory datasets but fail when illumination, shielding gas flow, or surface conditions change. Semi-supervised design utilizes unlabeled images to enrich the representation of real welding conditions, while the momentum teacher mechanism stabilizes the generation of pseudo-labels. The affinity field loss function encourages local consistency, so boundary pixels around welds and spatters are less prone to fragmentation. These design choices explain why the proposed method achieves a higher minimum intersection-union ratio than the contrastive model, even with a limited number of labeled samples. Another advantage of adaptive control strategies is that they combine data-driven prediction with rule-based interpretability. Neural networks can effectively approximate nonlinear relationships, but their outputs themselves do not clearly indicate how robots should safely adjust process parameters. Fuzzy control compensates for this deficiency by encoding expert-like rules. Negative errors and their variations do not simply produce arbitrary outputs; they correspond to meaningful decision directions for current, torch angle, and nozzle height. This is crucial for welding robots, as incorrect parameter corrections can lead to a momentary drop in weld quality. By limiting the adjustment range and using rule tables, the controller can keep the decision space within a physically reasonable range [30]. Source experiments also show that penetration depth and back fusion width should be controlled simultaneously. A weld may have a good surface appearance, but unstable root formation. Conversely, an excessive back fusion width may indicate excessive heat input, posing a risk of weld collapse. Therefore, the combined control of melt depth error and back fusion width error is more reliable than controlling a single response alone. BP neural networks use process parameters and molten pool geometry to estimate these responses, reflecting the fact that weld quality depends on the interaction between command parameters and actual thermofluid behavior. This multi-source input strategy is one reason why the controller can keep the back fusion width error within a specified range. Several issues need to be considered before industrial deployment. First, the camera and laser must be calibrated, as coordinate transformation errors will directly affect weld seam tracking. Secondly, the segmentation model should be updated when the production environment changes significantly, such as when the material surface condition, shielding gas, welding torch posture, or welding current range differs from the training conditions. Third, the output of the controller should be monitored through safety constraints in the robot controller and welding power source. Fourthly, the method should be tested on longer welds, curved welds, and multi-pass welds, as heat accumulation and interlayer geometry may be more complex in these cases than in single-pass welds.

6.6 Comparison with Conventional Robotic Welding

Unlike traditional robotic welding or “teach-repeat” style of operation, the methodology introduced here takes the robot’s role from one of a repetitive actuator to that of an intelligent executor of the welding process. Most of the intelligence involved in the conventional mode resides outside of the robot and is programmed into the robot by the human operator before the actual welding occurs [31]. The robot will follow the trajectory taught and use fixed parameters regardless of the fact the joint conditions may have changed from when the robot was programmed until the time it begins the actual welding process. In the new mode of operation, all of the knowledge relative to the welding process is embedded in the planning model, and visual data is interpreted by the segmentation network, while any deviation in welding quality is accounted for by an adaptive controller [32]. The robot is, therefore, capable of responding to the actual conditions of the joint being welded while carrying out the welding operation, therefore eliminating the necessity of relying solely upon the pre-weld preparation. Compared with the traditional method of optimizing the parameters, the new method has a greater degree of process robustness [33]. While taking the steps necessary to optimize parameters provides good starting points for the welding operation, it will not eliminate the disturbances that may occur due to the following factors: gap variation; heat/deformation; spatter/instability; and lastly, lack of. Conversely, a control-based method without

optimized initial parameters will generate a large amount of repair and make operation very close to the point of becoming unstable. By combining the best of both parameter optimization and control, the new methodology decreases the level of dependence on the pre-weld preparation and the uncertainty associated with the process will provide an integrated design that can provide for high-quality robotic GMAW applications in Table 10.

Table 10. Comparison between conventional robotic welding and the proposed intelligent welding framework

Aspect	Conventional robotic welding	Proposed intelligent welding framework
Operating mode	Teach-and-repeat operation based on pre-programmed paths	Closed-loop operation based on planning, sensing, prediction, and control
Source of intelligence	Mainly depends on the operator's experience before welding	Embedded in process models, visual perception, and adaptive control algorithms
Welding trajectory	Fixed trajectory taught before production	Corrected in real time according to detected seam position
Process parameters	Usually fixed after offline setup	Initialized by optimization and adjusted online through control rules
Response to disturbances	Limited ability to respond to gap variation, deformation, or thermal distortion	Can respond to joint deviation and weld formation errors during welding
Quality monitoring	Mostly relies on post-weld inspection or operator observation	Uses online prediction of weld formation indicators
Adaptability	Suitable for stable high-volume production with little variation	More suitable for low-batch, variable, or quality-sensitive production
Main limitation	High dependence on accurate teaching and pre-weld preparation	Requires reliable sensing, model updating, calibration, and safety constraints

7 Conclusions

The study introduces a method of controlling welding processes using deep-learning techniques for GMAW robots that optimises the welding process. The method includes process planning, modelling the response surface, performing standardised multi-objective grey wolf optimisation, using a semi-supervised semantic segmentation system, visual seam tracking and spatter suppression, predicting the outcome of a weld using neural networks and fuzzy logic based adaptive control. Welds are characterised in this paper as being a non-destructive test and many weld types can be fabricated together including Q235 carbon structural steel butt joints. The authors developed a robotic GMAW architecture using an ABB IRB1410 robot equipped with a digital welding power source and active laser vision sensor to perform the experiments. An intelligent process planning approach was developed to define the relationships between welding parameters and weld geometry to provide a basis for selecting welding process parameters that take into consideration material, geometry and the specified quality grade of the weld. A deep learning perception system was developed based on an improved U2PL architecture, which segments the weld seam, laser stripe, molten pool, spatter and distortion points from input images. The approach achieves an mIoU of 85.72%, which is better than both GTA and DeepLabV3+ for this specific dataset. The electrochemical of the presented adaptive control method consists of using a BP neural network to determine the predicted penetration and back-side fusion width from the detected welding parameters, and then the fuzzy controller is used to adjust the welding current, torch angle and nozzle height to maintain the specified penetration and control the back-side width error to within ±0.5 mm. The main contribution of the study is the integration of offline process optimization and online adaptive control into one robotic welding framework. The framework reduces dependence on manual experience, improves visual guidance ability and supports real-time weld formation control. Future work should extend the method to more materials, thicker plates, variable groove

geometries and multi-pass welding. In addition, large-scale industrial validation and real-time deployment on embedded edge-computing hardware will be necessary for broader manufacturing applications.

8 Acknowledgement

Continuous Mold Process Analysis and Mold Structure Optimization of the Lower Crossbeam of the Rear Seats in Automobiles, Project Number: 2024ZC050.

References

[1] Y.-K. Ma, J.-F. Fan, J. Hou, Y.-C. Fu, R. Tao, S. Wang, Vision-based autonomous robotic arc welding: State-of-the-art review and perspectives, IEEE Transactions on Automation Science and Engineering 22(2025) 21651-21673. https://doi.org/10.1109/TASE.2025.3614992

[2] K. Zhang, Z.-J. Yang, The effects of welding process parameters on properties of welded joint for enhancing welding structural integrity using simulation and experimental methods, Journal of Materials Research and Technology 38(2025) 2113-2125. https://doi.org/10.1016/j.jmrt.2025.08.067

[3] Z. Jin, R.-M. Marian, J.-S. Chahl, Achieving batch-size-of-one production model in robot flexible assembly cells, The International Journal of Advanced Manufacturing Technology 126(2023) 2097-2116. https://doi.org/10.1007/s00170-023-11246-y

[4] G.-Q. Liu, S.-Y. Han, X.-H. Tang, H.-C. Cui, Effects of torch configuration on arc interaction behaviors and weld defect formation mechanism in tandem pulsed GMAW, Journal of Manufacturing Processes 62(2021) 729-742. https://doi.org/10.1016/j.jmapro.2021.01.007

[5] I. Bunaziv, C. Dørum, S.-E. Nielsen, P. Suikkanen, X. Ren, B. Nyhus, M. Eriksson, O.-M. Akselsen, Root formation and metallurgical challenges in laser beam and laser-arc hybrid welding of thick structural steel, The International Journal of Advanced Manufacturing Technology 116(2021) 561-578. https://doi.org/10.1007/s00170-021-07453-0

[6] T. Talaei Khoei, H. Ould Slimane, N. Kaabouch, Deep learning: systematic review, models, challenges, and research directions, Neural Computing and Applications 35(2023) 23103-23124. https://doi.org/10.1007/s00521-023-08957-4

[7] T. Fredriksson, J. Bosch, H.-H. Olsson, An empirical evaluation of deep semi-supervised learning, International Journal of Data Science and Analytics 20(2025) 4127-4148. https://doi.org/10.1007/s41060-024-00713-8

[8] R. Yu, Y. Cao, J. Martin, O. Chiang, Y.-M. Zhang, Robotizing double-electrode GMAW process through learning from human welders, Journal of Manufacturing Processes 109(2024) 140-150. https://doi.org/10.1016/j.jmapro.2023.12.008

[9] B. Wang, S.-J. Hu, L. Sun, T. Freiheit, Intelligent welding system technologies: State-of-the-art review and perspectives, Journal of Manufacturing Systems 56(2020) 373-391. https://doi.org/10.1016/j.jmsy.2020.06.020

[10] A. Biber, R. Sharma, U. Reisgen, Robotic welding system for adaptive process control in gas metal arc welding, Welding in the World 68(2024) 2311-2320. https://doi.org/10.1007/s40194-024-01756-y

[11] J. Le, Y.-C. Liu, Y.-S. He, H. Zhang, X.-Q. Chen, Detection of wire feeding speed and its influence on rotating arc welding quality, The International Journal of Advanced Manufacturing Technology 125(2023) 5419-5429. https://doi.org/10.1007/s00170-023-11061-5

[12] W.-Q. Wang, W. Liu, Y. Zhang, Y. Liu, P.-D. Zhang, Z.-Y. Jia, Precise measurement of geometric and physical quantities in cutting tools inspection and condition monitoring: A review, Chinese Journal of Aeronautics 37(4)(2024) 23-53. https://doi.org/10.1016/j.cja.2023.08.011

[13] A. Beckers, L. Stauder, T. Grünebaum, S. Barth, T. Bergs, Design of economically-optimized manufacturing process sequences using cross-process models, CIRP Journal of Manufacturing Science and Technology 33(2021) 15-29. https://doi.org/10.1016/j.cirpj.2021.02.008

[14] Q.-W. Xu, Y.-X. Li, C. Zhang, Z.-D. Kou, A hybrid ResNet-LSTM model for real-time welding defect prediction and optimization, in: Proc. of the 2025 5th International Conference on Internet of Things and Machine Learning 25, 2025. https://doi.org/10.1145/3749566.3749574

[15] Y. Tong, G.-Z. Quan, H.-T. Wang, W. Xiong, Optimization of welding parameters using an improved hill-climbing algorithm based on BP neural network for multi-bead weld smoothness control, Materials 18(17)(2025) 4084.1-4084.27.

https://doi.org/10.3390/ma18174084
[16] R. Ali, A. El-Betar, M. Magdy, A review on optimization of autonomous welding parameters for robotics applications, The International Journal of Advanced Manufacturing Technology 134(2024) 5065-5086. https://doi.org/10.1007/s00170-024-14396-9.
[17] H.-C. Wang, Y.-C. Wang, Y.-J. Shen, J.-S. Fan, Y.-X. Wang, Z.-X. Zhang, Using unreliable pseudo-labels for label-efficient semantic segmentation, International Journal of Computer Vision 133(2025) 1476-1498. https://doi.org/10.1007/s11263-024-02229-x.
[18] C. Pabba, P. Kumar, A vision-based multi-cues approach for individual students and overall class engagement monitoring in smart classroom environments, Multimedia Tools and Applications 83(2024) 52621-52652. https://doi.org/10.1007/s11042-023-17533-w.
[19] N. Yang, F. Huang, D. Yuan, AdaptMatch: Adaptive consistency regularization for semi-supervised learning with top-k pseudo-labeling and contrastive learning, AI 2023: Advances in Artificial Intelligence, Lecture Notes in Computer Science 14471(2024) 227-238. https://doi.org/10.1007/978-981-99-8388-9_19.
[20] D. Baek, H.-S. Moon, Robust laser vision sensing technology for adaptive weld seam tracking in shipbuilding automation, The International Journal of Advanced Manufacturing Technology 139(2025) 2003-2026. https://doi.org/10.1007/s00170-025-15896-y
[21] Z. Zeng, Y.-C. Yang, J.-R. Yuan, B.-J. Qi, Dynamic prediction of backside weld width: factor analysis and progressive deep learning enhancements, Welding in the World 69(2025) 3053-3069. https://doi.org/10.1007/s40194-025-02024-3
[22] B. Xue, B.-H. Chang, D. Du, Multi-output monitoring of high-speed laser welding state based on deep learning, Sensors 21(5)(2021) 1626.1-1626.15. https://doi.org/10.3390/s21051626
[23] B. von Querfurth, S.-E. Belhout, C. Knaak, S. Mann, P. Abels, C. Holly, J. Tatman, D. Barborak, M. Hargadine, AI-driven autonomous adaptative feedback welding machine, Welding in the World 69(2025) 1419-1426. https://doi.org/10.1007/s40194-024-01898-z
[24] B. Denkena, M. Wichmann, K.M. Heide, F. Wiesener, H.N. Nguyen, Automated process planning in milling of hybrid components, Production Engineering 17(2023) 511-520. https://doi.org/10.1007/s11740-022-01180-5.
[25] H. Besharati-Foumani, M. Lohtander, J. Varis, Intelligent process planning for smart manufacturing systems: a state-of-the-art review, Procedia Manufacturing 38(2019) 156-162. https://doi.org/10.1016/j.promfg.2020.01.021.
[26] Z.-Y. Lu, R.-S. Gu, H.-M. Cheng, M.-Y. Xu, P.-F. Xu, Y. Kinoshita, J. Ye, G.-Y. Jia, Q. Wu, Unlabeled data augmentation with diffusion model for semi-supervised object detection, The Visual Computer 41(2025) 11767-11782. https://doi.org/10.1007/s00371-025-04103-4.
[27] E. Bodden, J. Pottebaum, M. Fockel, I. Gräßler, Evaluating security through isolation and defense in depth, IEEE Security & Privacy 22(2024) 69-72. https://doi.org/10.1109/MSEC.2023.3336028.
[28] Z.-Y. Yan, C. Liu, T.-M. Li, Z. Ma, Y.-Y. Wu, Y.-C. Cheng, S.-J. Chen, Autonomous optimization technology for welding parameters based on a dual-driven model incorporating physics and data, Journal of Manufacturing Processes 135(2025) 131-141. https://doi.org/10.1016/j.jmapro.2025.01.019.
[29] J. Backman, V. Kyllönen, H. Helaakoski, Methods and tools of improving steel manufacturing processes: current state and future methods, IFAC-PapersOnLine 52(2019) 1174-1179. https://doi.org/10.1016/j.ifacol.2019.11.355.
[30] R. Ali, A. El-Betar, M. Magdy, A review on optimization of autonomous welding parameters for robotics applications, The International Journal of Advanced Manufacturing Technology 134(2024) 5065-5086. https://doi.org/10.1007/s00170-024-14396-9.
[31] J.-T. Licardo, M. Domjan, T. Orehovački, Intelligent Robotics—A Systematic Review of Emerging Technologies and Trends, Electronics 13(3)(2024) 542.1-542.44. https://doi.org/10.3390/electronics13030542.
[32] M. Asadi, A. Ashoori, M. Afshar, A. Sheikhshab, T. Scheerer, A. Kaspardlov, S. Bagheri, S. Firouz, S. Karimzadeh, Vision-driven adaptive welding solutions for the top three challenges in welding fabrication, Welding in the World 69(2025) 1277-1289. https://doi.org/10.1007/s40194-025-01968-w.
[33] R. Ali, A. El-Betar, M. Magdy, A review on optimization of autonomous welding parameters for robotics applications, The International Journal of Advanced Manufacturing Technology 134(2024) 5065-5086. https://doi.org/10.1007/s00170-024-14396-9.